THE ASTROPHYSICAL JOURNAL, 341:474–483, 1989 June 1

CORONAL ACTIVITY IN F-, G-, AND K-TYPE STARS. III. THE CORONAL DIFFERENTIAL EMISSION MEASURE DISTRIBUTION OF CAPELLA, σ^2 CrB, AND PROCYON

J. R. LEMEN
Lockheed Palo Alto Research Laboratory

R. MEWE
Laboratory for Space Research, Utrecht, The Netherlands

C. J. SCHRIJVER
Joint Institute for Laboratory Astrophysics, University of Colorado and National Bureau of Standards

AND

A. FLUDRA
Astronomical Institute, Wroclaw University, Poland
Received 1988 July 13; accepted 1988 November 9

ABSTRACT

EXOSAT soft X-ray spectra of three binary systems of cool stars are analyzed: Capella (G6 III + F9 III), σ^2 CrB (F8 V + G1 V), and Procyon (F5 IV-V + DF) (the candidate X-ray emitters are underlined). The *EXOSAT* transmission grating spectrometer permits the study of individual spectral lines and line complexes between 10 Å and 200 Å with approximately 3 Å resolution. First we demonstrate that the spectra can be described reasonably well by a two-temperature model corona. Then we relax the assumption that only two temperatures exist in the stellar coronae and derive differential emission measure distributions from the three spectra. The results from the multithermal modeling are consistent with those of the two-temperature models: emission from the coronae of each of the three stars is dominated by plasma in two relative narrow temperature intervals. These intervals are centered on 5 MK and 25 MK in the cases of Capella and σ^2 CrB, and 0.6 MK and 3 MK in the case of Procyon. The implications of the results for the structure of stellar coronae are briefly discussed.

Subject headings: line identifications — stars: corona — stars: late-type — stars: X-rays — X-rays: spectra

I. INTRODUCTION

The imaging proportional counter (IPC, see Gorenstein, Harnden and Fabricant 1981) of the *Einstein HEAO 2* observatory demonstrated that soft X-ray emitting coronae are a common feature among stars on the cool side of the Hertzsprung-Russell diagram. Although limited spectral information was available for the brighter X-ray sources observed with the IPC, the poor spectral resolution ($\Delta E/E \approx 100\%$) and limited wavelength range (3–60 Å, or 0.2–4 keV) of the IPC did not allow a detailed determination of the temperature structure of the coronae. Single-temperature fits, however, did provide estimates of the mean, or characteristic, coronal temperatures. Typical mean temperatures for stellar coronae range from 2 MK up to 50 MK (Schrijver, Mewe, and Walter 1984; hereafter Paper II). The IPC observations of some of the brightest stellar sources show that the coronae of these stars cannot be isothermal, so that at least two components must exist with different temperatures and emission measures. Therefore, Paper II tentatively concludes that (at least) two dominant temperatures exist in stellar coronae: a moderately hot component around 4 MK and a high-temperature component around 20 MK. The ratio of emission measures corresponding to these two components can differ markedly from star to star. The stellar parameters determining the ratio of the emission measures for these two components were not determined.

The first high-resolution X-ray spectra of nonsolar coronae were obtained with the objective grating spectrometer (OGS) and the solid state spectrometer (SSS) on *Einstein* (see, e.g., Swank *et al.* 1981; Mewe *et al.* 1982). Although the spectral resolution of these instruments was much better than that of the IPC, the wavelength ranges of both instruments were rather limited. Most of the observations obtained with these spectrometers gave clear evidence for two or more temperatures in stellar coronae. Majer *et al.* (1986), for instance, find evidence for at least two temperature components in a number of IPC spectra of RS CVn type binaries. Their study, however, shows that the instrumental properties of the IPC are such that two temperature ranges (around 3 and 15 MK) are most likely to be found in a two-temperature fit, even if there would be a significant contribution at other temperatures.

More recently, high-resolution X-ray spectra have been obtained with the transmission grating spectrometer (TGS) on the *EXOSAT* spacecraft. The TGS permits the study of individual spectral lines and line complexes over a wide wavelength range from 10 to 200 Å with approximately 3 Å resolution. In an earlier study of the *EXOSAT* spectra, Schrijver (1985) showed that the spectra of Capella, σ^2 CrB, and Procyon can be adequately described by a two-temperature model: 3 MK and 18 MK in the case of Capella and σ^2 CrB, and 0.7 MK and 2.5 MK in the case of Procyon (note that he used a spectral model that differed somewhat from the final version we use here, causing the temperatures resulting from the fits to be slightly different). These results appear to agree with the basic conclusion from Paper II, although the Procyon data introduce a third, cool plasma component that is not found in the sample of IPC spectra studied in Paper II.

The two-temperature fits to the *EXOSAT* spectra provide a

reasonably good description of the observed line strengths, although a formal error analysis shows that the acceptance levels are quite low in the case of Capella (see § IV). One would like to be certain, however, that the two-temperature result is indicative of a fundamental characteristic of stellar coronae and not merely an artifact of the adopted four-parameter model (fitting two temperatures and two emission measure values). If, for example, a multithermal model can be shown to reproduce the fits with a similar statistical acceptance as the two-temperature model, the interpretation of the spectra in terms of just two dominant temperatures is not unique, and may be incorrect. On the other hand, if a multithermal analysis can be shown to be in general agreement with the two-temperature fits, one can make a strong case for a two-temperature interpretation. The combination of two-temperature and multithermal analyses of the coronal spectra will increase our knowledge of the detailed temperature structure of the atmospheric plasma, and may thus place constraints on the geometry, the dynamics, and the heating of stellar coronae. Therefore, we perform a detailed multithermal analysis of the *EXOSAT* TGS spectra of the cool stars Capella, σ^2 CrB, and Procyon (earlier reports of the observations were given by Mewe 1984; Brinkman *et al.* 1985; Schrijver 1985; Schrijver and Mewe 1986; and Mewe *et al.* 1986). We relax the assumption that the stellar coronae contain material at only two-temperatures and derive differential emission measure distributions.

The theoretical spectra are described in § II. The observations are reviewed in § III and a two-temperature model is discussed in § IV. The methods used to perform the multi-temperature modeling are described in § V*a* and the results presented in § V*b*. The discussion and summary of conclusions are presented in § VI.

II. THEORETICAL X-RAY SPECTRA

A comparison of observed and theoretical spectra can provide estimates of the plasma parameters such as temperature, emission measure, elemental abundances, the degree of ionization equilibrium, and can place limits on the column density of the intervening plasma. During the past decade we have developed a theoretical model for spectra emitted by hot, optically thin plasmas (e.g., Mewe 1972; Mewe and Gronenschild 1981; Mewe, Gronenschild, and van den Oord 1985; Mewe, Lemen, and van den Oord 1986). For the purpose of the present study, we calculated a library of theoretical spectra and convolved these with the response and resolution characteristics of the *EXOSAT* TGS with the 3000 Å Lexan filter. We used the spectral code of Mewe, Gronenschild, and van den Oord (1985) and Mewe, Lemen, and van den Oord (1986) for an optically thin and isothermal plasma with cosmic abundances (as given by Allen 1973) and interstellar hydrogen column densities N_H ranging from 10^{18} to 10^{19} cm^{-2}. We have used a grid of 67 temperatures between 0.5 and 100 MK, spaced by intervals $\Delta \ln T(\mathrm{K}) = 0.081$. We assume that the plasma is in steady-state ionization equilibrium, that the electron energy distribution is Maxwellian, and that the intensities of the dominant lines are independent of electron densities in the stellar coronae (e.g., $n_e < 10^{12}$ cm^{-3}).

Figure 1 shows a few examples of spectra calculated for temperatures $T = 0.6$, 2, 5.1, and 20 MK. The ion species of several of the strongest lines are identified. The spectra are convolved with the response function of the *EXOSAT* TGS, which incorporates the effective instrumental area and the wavelength resolution function of the grating and the detector. We note that the intrinsic spectral line broadening is negligible compared to the instrumental width. The correspondence between the appearance of certain spectral lines and the temperature at which they have their peak emission is shown in Figure 2.

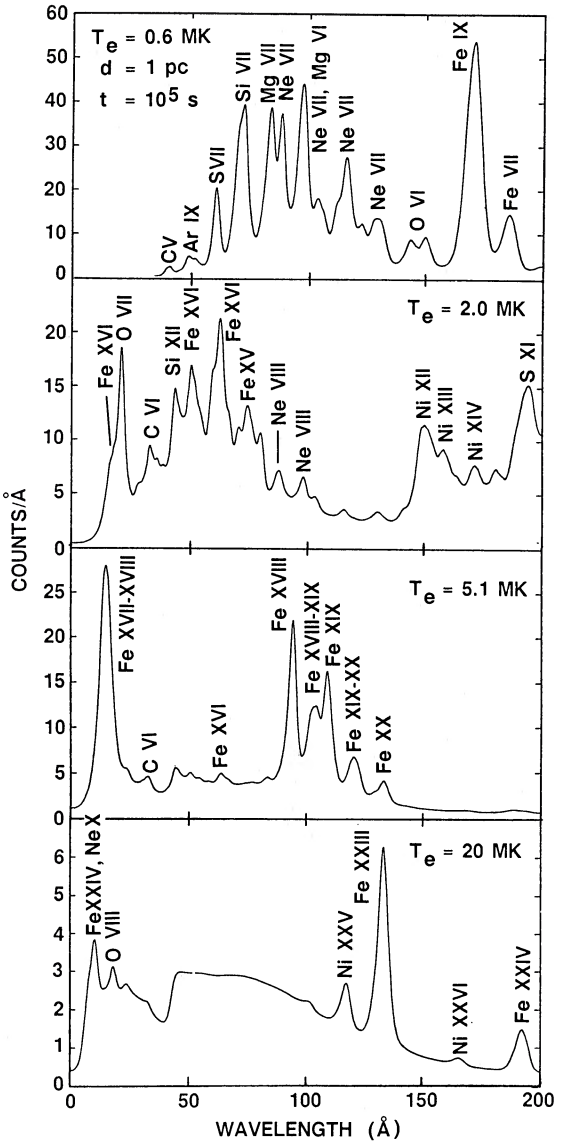

FIG. 1.—Examples of theoretical spectra, folded with the *EXOSAT* response function and given in 1 Å bins. The most prominent lines are labeled with the corresponding ion species. Panels *a*, *b*, *c*, and *d* are for temperatures $T = 0.6$, 2.0, 5.1, and 20 MK and for interstellar hydrogen column densities $N_H = 2$, 2, 5, and 5 ($\times 10^{18}$ cm^{-2}), respectively. The emission measure equals $EM = 10^{50}$ cm^{-3}, the source distance $d = 1$ pc, and the observation time $t = 10^5$ s.

III. OBSERVED SOFT X-RAY SPECTRA

Three X-ray spectra of cool stars were obtained with the *EXOSAT* 500 lines per mm transmission grating in conjunction with the (3000 Å) Lexan filter, and the channel multiplier array in the focal plane of a grazing incidence telescope. De Korte *et al.* (1981), Brinkman *et al.* (1980), and Mewe (1984)

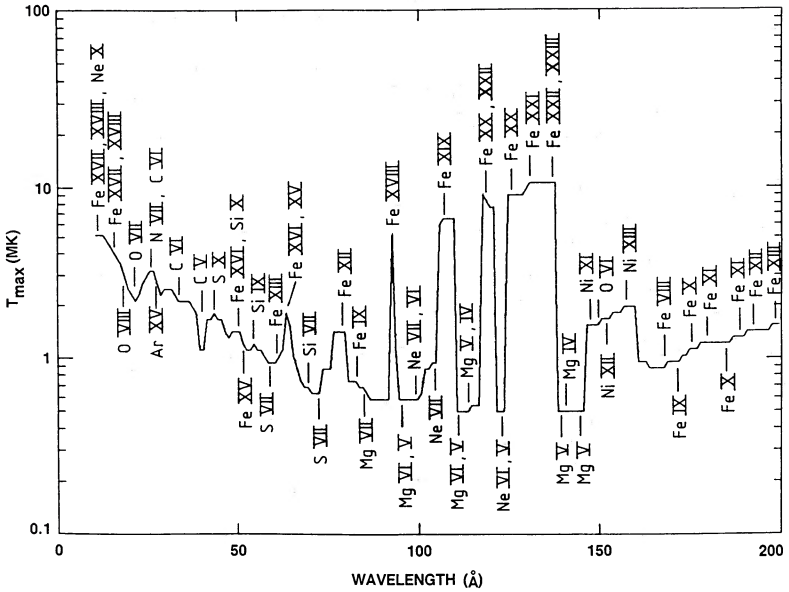

FIG. 2.—Temperature T_{max} at which the maximal intensity is reached in 1 Å bins as a function of wavelength. The ion species that contribute most strongly to the intensity at T_{max} are identified.

describe the instrument. The observation dates, exposure times, and relevant source data are given in Table 1.

The light curves for Capella and σ^2 CrB as observed by the *EXOSAT* low-energy (LE) instrument and by the medium-energy (ME) proportional counter array of eight detectors (see Turner, Smith, and Zimmermann 1981) are shown in Figure 3. The temporal variations in the integrated X-ray flux are generally small. Some of the slow changes may be caused by the stellar rotation which causes individual active regions to rotate onto and behind the stellar disk. The binary σ^2 CrB showed a strong flare that lasted approximately 3 hours (see Brinkman *et al.* 1985; van den Oord, Mewe, and Brinkman 1988*a*, *b*). The time interval during which the flare occurred is excluded from the present analysis. The differences between the σ^2 CrB spectra recorded by the ME during the first 13.9 hours of the observation (before the flare) and during the last 6.9 hours after the flare do not differ significantly (see van den Oord, Mewe, and Brinkman 1988*a*, *b*). Therefore, we think it unlikely that the energy released in the flare significantly heats the corona in the hours after the flare decay phase.

The observed spectra are shown as histograms in Figure 4. The right and left higher orders have been averaged, and the spectra have been corrected for an average background (Table 1), and rebinned by a factor of 5 in 2.5 Å bins (for Procyon in 5 Å bins).

The intensity between 50 Å and 70 Å in the left spectral order is slightly higher than in the corresponding part of the right spectral order in the spectra of all three sources (see Fig. 4 in Brinkman *et al.* 1985). This may be attributed to statistically allowed differences in the counting rates or to a position-dependent change in the detector response. We cannot distinguish between these two alternatives, and thus the reality of the features in this spectral range is uncertain. Note that the spectral fits described in the next section do not agree with this particular part of the spectrum very well, which may reflect the fact that the features in either the right or left higher order spectra are affected by an unknown instrumental effect.

Some interesting points readily emerge from an identification of spectral lines and line complexes. The two most active stars, Capella and σ^2 CrB, show a prominent Fe XXIII line at 133 Å which is typical for hot plasmas of about 10–20 MK, such as observed in solar flares (Kastner, Neupert, and Swartz 1974; Mason *et al.* 1984). This hot line is absent in the Procyon spectrum, which contains instead a strong blend of lines around 170 Å, that can be identified as lines from Fe IX–XI ions; Fe IX–XI ions are formed in a cool corona with a temperature between 0.6 and 2 MK. The absence of the 170 Å emission feature in the spectra of Capella or σ^2 CrB implies that relatively little plasma cooler than 2 MK can be present. This conclusion is supported by the narrowness of the Fe XVII–

TABLE 1

SOURCE DATA

Source	Spectral[a] Type	Dist.[b] (pc)	N_H (10^{18} cm^{-2})	Ref.	Obs. Date (1983)	Eff. Exposure Duration (10^4 s)	Background (cts/Å)
Capella (α Aur)	G5 III+F9 III	13.2	5	1,2	Oct 24/25	8.49	20.4
σ^2 CrB	F8 V+G1 V	23.	5	1,3	Sep 28/29	8.06	16.6
Procyon (α CMi)	F5 IV–V+DF	3.5	2	1,2	Oct 21/22	2.14	4.9

[a] Candidate X-ray emitter underlined.

[b] Hoffleit and Jaschek (1982).

REFERENCES.—(1) Paresce 1984; (2) Dupree 1981; (3) Tarafdar and Agrawal 1984.

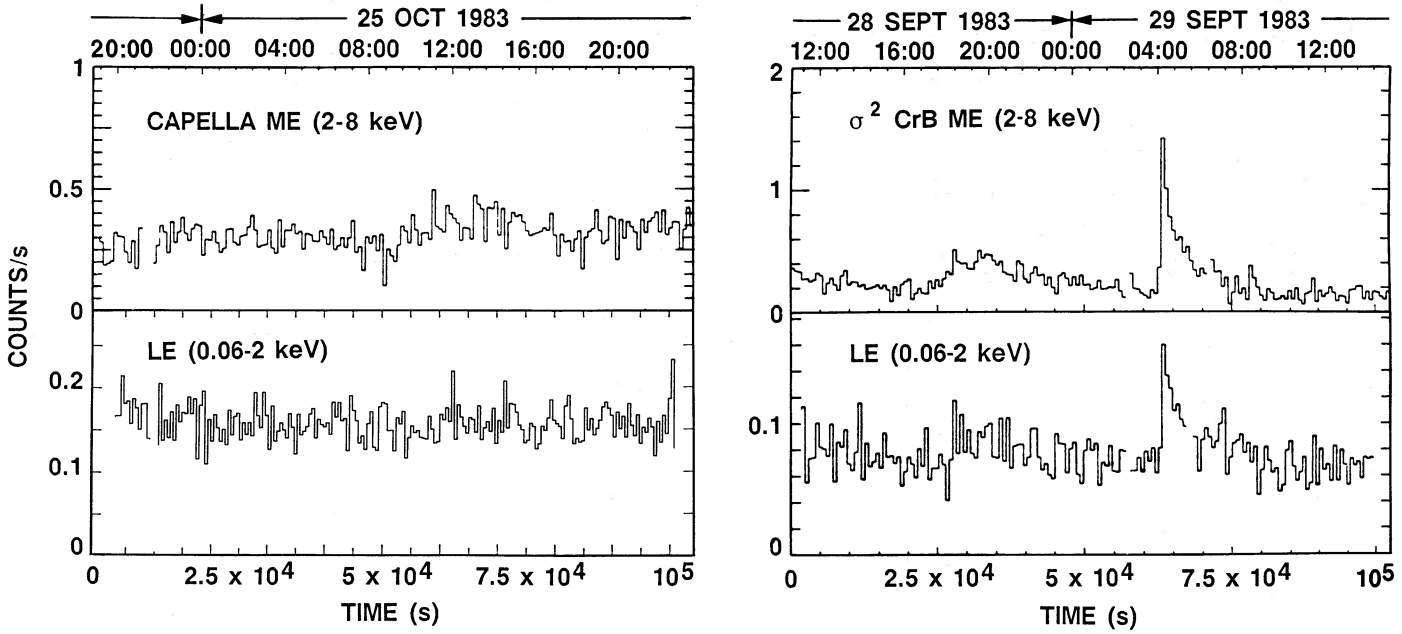

FIG. 3.—Background-corrected light curves of Capella and σ^2 CrB as obtained with the medium-energy detector (ME count rate is per detector element of the array) and as derived from the zeroth-order part of the low-energy (LE) TGS spectrum. The data are binned in 480 s intervals for the ME and in 500 s intervals for the LE. The data for Capella before 21:38 UT of October 24 are not used in our spectral analysis. The flare between 04:02 and 06:47 UT of September 29 in the spectral data of σ^2 CrB is also excluded.

XVIII line complex at 15 Å: if much plasma with temperatures below 2 MK were present, this complex would be broadened by a significant contribution from O VII lines at 21.1 Å. The intensity ratio of the 15 Å line complex and the Fe XVIII–XXIII complex between 90 Å and 140 Å demonstrates that the spectra cannot be emitted by an isothermal plasma (see § IV).

IV. ONE- AND TWO-TEMPERATURE SPECTRAL FITS

A simple first approach to the modeling of the spectra is to compare the observed spectra with the model of an isothermal plasma. It turns out that a single-temperature fit gives unacceptably large χ^2 values for all the spectra considered. The spectrum of an isothermal plasma cannot describe all of the observed lines, as shown by the best-fit case for Capella in Figure 5. Hence, a one-temperature interpretation is ruled out, except possibly for the case of Procyon where the acceptance level for the one-temperature fit is 70% (reduced minimum $\chi_\nu^2 = 0.9$, for $T = 0.6$ MK and emission measure $EM = 4.6 \times 10^{50}$ cm^{-3}).

Figure 4 allows a comparison between the observed spectra of Capella, σ^2 CrB, and Procyon and the best-fit two-temperature simulated spectra. Overall agreement is obtained between theoretical and observed spectra. The two-temperature fits (Table 2) have acceptance levels of 1, 95, and 95% for Capella, σ^2CrB, and Procyon, respectively. The fits suggest that for Capella and σ^2 CrB the coronal radiative losses occur predominantly around temperatures of 5 MK and 22 MK. In addition to a 2 MK component comparable to the cool component on Capella and σ^2 CrB, the Procyon spectrum fit requires a cooler component of approximately 0.6 MK.

Thus, the two-temperature model is in reasonable agreement with the observed spectra of the three stars, although only the fits to the σ^2 CrB and Procyon spectra meet statistical acceptance criteria. In the next section we relax the two-temperature assumption and attempt to model X-ray spectra in terms of a more general differential emission measure distribution.

V. DIFFERENTIAL EMISSION MEASURE ANALYSIS

a) Theory

For a multithermal plasma the (line + continuum) spectral intensity $f(\lambda_j)$ (counts s^{-1}) measured at Earth by the TGS in wavelength bin λ_j may be expressed as

$$f(\lambda_j) = \frac{1}{4\pi d^2} \int F(\lambda_j, T)\varphi(T)dT \,, \tag{1a}$$

or, integrated logarithmically:

$$f(\lambda_j) = \frac{1}{4\pi d^2} \int F(\lambda_j, T)T\varphi(d\ln T) \,, \tag{1b}$$

TABLE 2

TWO-TEMPERATURE FITS TO *EXOSAT* TGS SPECTRA[a]

Source	T_1 (MK)	EM_1 (10^{51} cm^{-3})	T_2 (MK)	EM_2 (10^{51} cm^{-3})	EM_1/EM_2	χ_ν^2	ν (d.o.f.)	Acceptance Level A(%)
Capella	4.7	55	22	180	0.31	1.4	74	1
σ^2 CrB	6.1	65	24	420	0.16	0.7	74	95
Procyon	0.5	0.73	2	1.5	0.49	0.6	36	95

[a] Shown are the temperatures and the emission measures for the two-temperature fits, the ratio of emission measures, the reduced χ^2 values, the number of degrees of freedom (d.o.f.), and the acceptance level A of the fit.

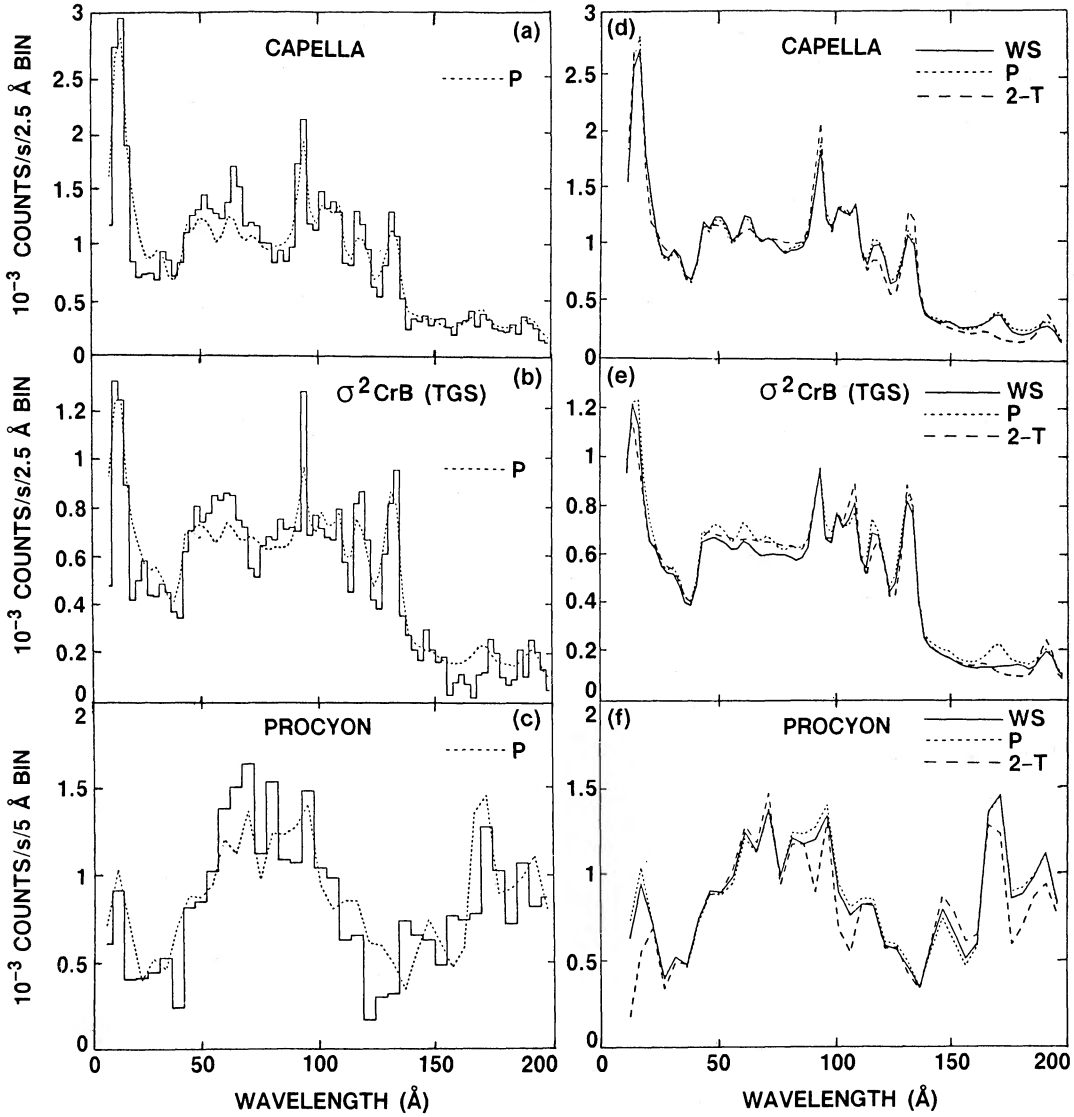

FIG. 4.—*EXOSAT* 500 lines per mm TGS spectra of (*a*) Capella, (*b*) σ^2 CrB, and (*c*) Procyon compared with the "polynomial" (*P*) best fit (see § V*a* for a description of analysis techniques). Panels *d*, *e*, and *f* give best-fit spectra, comparing: (1) two-temperature fit spectrum, (2) "polynomial" (*P*) fit spectrum, and (3) "Withbroe-Sylwester" (WS) fit spectrum. The spectra in panels *a*, *b*, *d*, and *e* are given in 2.5 Å bins; in panels *c* and *f* in 5 Å bins.

where $F(\lambda_j, T)$ is the spectral emissivity (counts cm^5 s^{-1}) for the line plus continuum emission as a function of temperature T integrated over wavelength bin λ_j, convolved with the TGS instrumental response function. The distance to the source is d (cm), and $\varphi(T)$ (cm^{-3} K^{-1}) is given by

$$\varphi(T)dT = {n_e}^2 dV , \tag{2}$$

where n_e is the electron density (cm^{-3}) and V the plasma volume (cm^3). Note that the total emission measure is given by $EM = \int T\varphi(T)d(\ln T) = \int {n_e}^2 dV$. We shall use the term differential emission measure distribution interchangeably for $\varphi(T)$ and $T\varphi(T)$, only specifying which of these is meant where ambiguities would otherwise arise. We consistently use $T\varphi(T)\Delta \ln(T)$ in the graphic representations in this paper.

The differential emission measure distribution can be derived from the observed spectrum by deconvolving $\varphi(T)$ from the measured spectral intensities $f(\lambda_j)$, using known emission functions $F(\lambda_j, T)$ for the individual wavelength bins (see § II). For this deconvolution we apply two different iterative techniques which both use an initial form for the differential emission measure, $\varphi_0(T)$, to calculate theoretical line intensities. The comparison of observed and theoretical line intensities yields a new $\varphi_1(T)$. Subsequent iterations are performed to minimize the value of χ^2 given by

$$\chi^2 = \sum_{j=1}^{N} \frac{[f_O(\lambda_j) - f_C(\lambda_j)]^2}{\sigma^2(\lambda_j)} , \tag{3}$$

where, $f_O(\lambda_j)$ and $f_C(\lambda_j)$ are the observed and computed inten-

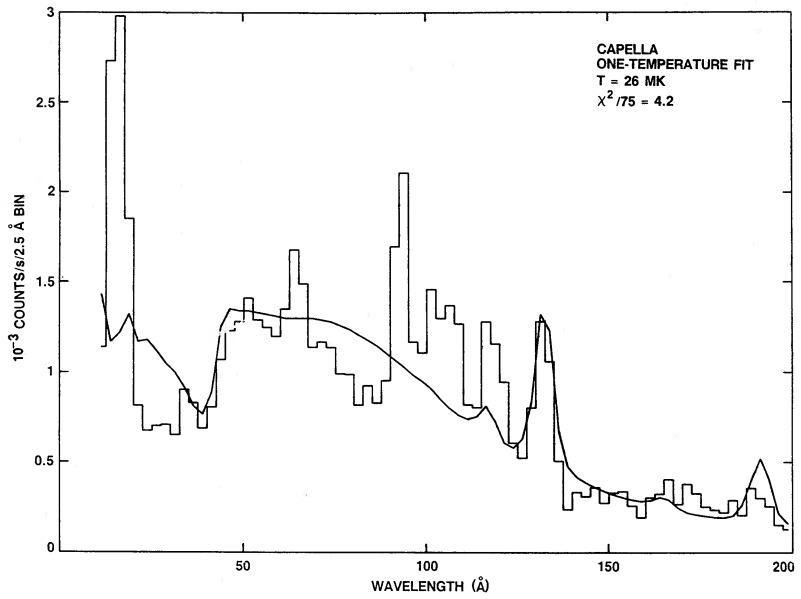

FIG. 5.—Single-temperature fit to Capella spectrum (given in 2.5 Å bins). The observed spectrum is given as a histogram, the best-fit spectrum as a smooth curve. The best-fit parameters (for a fixed value $N_H = 5 \times 10^{18}$ cm^{-2}) are given in the top-right corner.

sities in wavelength bin λ_j, $\sigma(\lambda_j)$ is the statistical error in the observed count rate, and the summation over j corresponds to the total of N wavelength bins in the observed spectrum.

The crucial step in the iteration procedure is the determination of the new form for the differential emission measure distribution $\varphi_{i+1}(T)$ based on the comparison of calculated and observed line intensities during the ith iteration. We apply two different algorithms. The first method—the Withbroe-Sylwester (WS) technique—is based on a weighting-factor method originally proposed by Withbroe (1975), and modified by Sylwester, Schrijver, and Mewe (1980). This technique computes the next approximation of the differential emission measure distribution, $\varphi_{i+1}(T)$, from the previous one, $\varphi_i(T)$, by

$$\varphi_{i+1}(T) = \varphi_i(T) \frac{\sum_{j=1}^{N} W_j(T) f_O(\lambda_j)/f_C(\lambda_j)}{\sum_{j=1}^{N} W_j(T)}, \quad (4)$$

where, $f_O(\lambda_j)$ and $f_C(\lambda_j)$ are defined above. Sylwester, Schrijver, and Mewe (1980) derived a semiempirical expression for the empirical weighting function $W_j(T)$, which takes into account the uncertainties, $\sigma(\lambda_j)$, in the measurements of the observed intensities. This method makes no assumptions about the functional form of the differential emission measure distribution (in principle there are N degrees of freedom), although the final result is subject to an implicit smoothing because the weighting functions contain integrals over the entire spectral range (Fludra and Sylwester 1986).

The second approach—the polynomial (P) method—was suggested by Bruner *et al.* (1989) who assumed that the shape of $\varphi(T)$ can be approximated by the exponential of a polynomial given by

$$\varphi(T) = \alpha e^{\omega(T)}, \quad (5)$$

where α is a normalization constant and $\omega(T)$ is a polynomial function of temperature. In the subsequent discussion we refer to this method as the polynomial technique. For convenience, we have followed the suggestion of Bruner *et al.* (1989) and have chosen

$$\omega(T) = \sum_{k=1}^{M} a_k P_k(T),$$

where P_k is a Chebyshev polynomial of order k. This ensures that the coefficients, a_k, are all roughly the same order of magnitude and makes the search for the best solution over parameter space better conditioned. In principle, one should choose solutions with the lowest order polynomial which still provides an acceptable fit to the data. We use polynomials of order 9.

Applications of the above methods to solar X-ray spectra can be found in Withbroe (1975), Levine and Pye (1980), Sylwester, Schrijver, and Mewe (1980), Jakimiec *et al.* (1984), and Bruner *et al.* (1989).

The multithermal analysis technique should satisfy the general condition that $\varphi(T) \geq 0$. Craig and Brown (1976*a*, *b*), for example, have criticized the multithermal analyses of X-ray spectra based on a mathematical model which did not meet this criterion. Both of the described techniques are formulated to exclude *a priori* negative values for the emission measure.

b) Results of the Differential Emission Measure Analysis

The results of the multithermal differential emission measure analysis are presented in Figure 6 (see also Table 3 for χ^2 and acceptance levels). The differences between the results from the algorithms described in § V*a* are an indication of the uncertainties in determining $T\varphi(T)$. The resulting $T\varphi(T)$ for the two different algorithms are in good agreement for temperatures between 2 MK and 20 MK, for which pronounced spectral lines are available in the theoretical spectra (see Fig. 2). For comparison, the results of the two-temperature model are indicated in Figure 6.

Large discrepancies between the $T\varphi(T)$ curves from the two algorithms for each of the stars occur at temperatures below 3 MK (Fig. 6). The spectral range between 160 Å and 200 Å contains line features that are sensitive to temperatures down

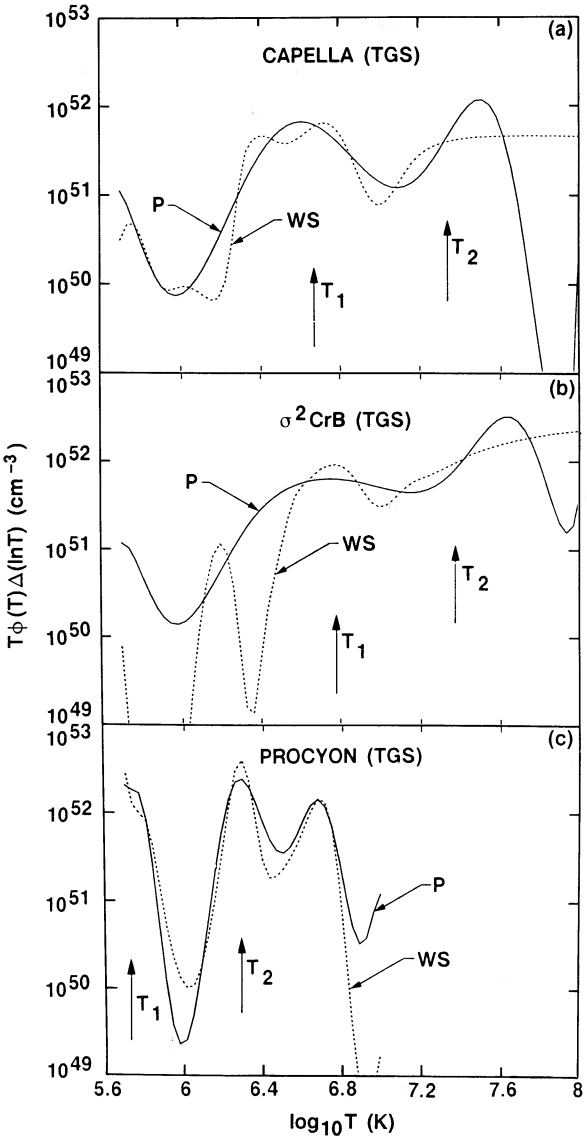

FIG. 6.—The differential emission measure curves [$DEM = T\varphi(T)\Delta \ln(T)$, with $\Delta \ln(T) = 0.081$] (*a*) for Capella, (*b*) σ^2 CrB, and (*c*) Procyon. Each panel contains the result of the "Withbroe-Sylwester" (WS) method (*dotted*) and of the "polynomial" (*P*) method (*solid*). Two arrows in each panel mark the results of the two-temperature fits (Table 2).

to 0.5 MK. The observed intensities, however, are small and have a poor signal-to-noise ratio in this wavelength interval. Thus, the differences at low temperatures between the differential emission measure curves resulting from the two different algorithms are not statistically significant.

Strong disagreements between the two $T\varphi(T)$ models are also seen at temperatures above approximately 20 MK. This is caused by the absence of strong spectral lines characteristic of these high temperatures (see Fig. 2), and by the fact that the continuum changes only weakly as a function of temperature. Hence, the shape of the differential emission measure curve contains no significant information for temperatures above 20 MK and is not well constrained. In contrast to the TGS, the *EXOSAT* medium energy (ME) experiment is sensitive to emission from plasmas at temperatures above about 10 MK, although the spectral resolution is much lower. The ME spectra allow a fairly accurate temperature determination below approximately 40 MK, but can also distinguish between higher plasma temperatures, albeit with less precision. The ME and TGS spectra were analyzed jointly using both multithermal algorithms. The resulting differential emission measure at temperatures above 40 MK is reduced for both algorithms (see Fig. 7) and the results of the two methods are in better agreement than in the analysis of the TGS spectra only: the inclusion of the ME data helps to constrain the solution at the higher temperatures. As expected from the remarks given earlier in this paragraph, the TGS spectra that are predicted from these combined ME and TGS differential emission measure curves differ little from those resulting from the TGS data alone.

The characteristic features of the differential emission measure distributions are remarkably similar for the spectra of Capella and σ^2 CrB: there is a very steep increase with temperature up to 3 MK, followed by a "depression" around 10 MK, and another increase toward temperatures about 20 MK. To ensure that the "depression" in the differential emission measure around 10 MK is not artifact of the method, the differential emission measure curve from the Capella polynomial method with a "filled in" depression was generated, shown by the solid curve in Figure 8*a*. A synthetic spectrum was calculated from this artificial differential emission measure curve; we added noise to the synthetic spectrum similar to the noise in the observed Capella spectrum (histogram in Fig. 8*b*). The polynomial differential emission measure technique was applied to the synthetic spectrum to derive a curve for $T\varphi(T)$ (dashed curve in Fig. 8*a*) and a fitted spectrum (dashed curve in Fig. 8*b*). It can be seen from the figure that the polynomial

TABLE 3

RESULTS OF DIFFERENTIAL EMISSION MEASURE ANALYSIS[a]

SOURCE		TGS			TGS + ME		
		χ_ν^2	ν	A(%)	χ_ν^2	ν	A(%)
Capella	WS	1.04	76	38	1.04	96	37
	P	1.18	66	15	1.16	86	15
σ^2 CrB	WS	0.64	76	99	0.92	96	70
	P	0.74	66	94	0.89	86	76
Procyon	WS	0.46	38	>99	0.44	45	>99
	P	0.49	28	99	0.45	35	>99

[a] For Withbroe-Sylwester (WS) and polynomial (*P*) methods (see § V*a*). Shown are reduced χ^2 values, the number ν of degrees of freedom, and the statistical acceptance level A of the fit.

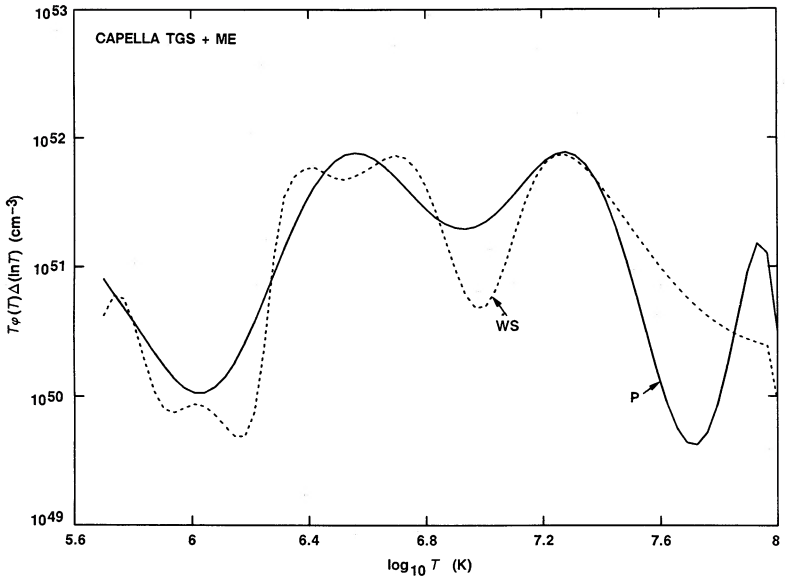

FIG. 7.—Differential emission measure curves for Capella for the combined TGS and ME spectral data. The results of the WS and *P* methods (see § V*a*) are given as a dotted and a solid line, respectively.

technique very successfully extracted the original artificial differential emission measure model, and matched the input spectrum. We conclude that the observed structure in the differential emission measure curve (Fig. 6*a*) is not an artifact of the method used to determine it. As expected from this result, the simulated spectrum is not compatible with the observed Capella spectrum (compare Fig. 8*b* and Fig. 4*a*).

Thus, the results of the differential emission measure analysis support the hypothesis that the spectra of Capella and σ^2 CrB are dominated by emission from plasma with temperatures in two narrow intervals, centered on the temperatures resulting from a best fit in a simple two-temperature model.

The differential emission measure distribution derived for Procyon (Fig. 6*c*) is more uncertain because of the poor signal-to-noise ratio of the spectrum. A relatively strong contribution is suggested from plasma at temperatures around 0.6 MK and at temperatures in the range between 2 and 6 MK (Schmitt *et al.* [1985] also find the latter temperature component in the IPC spectrum of Procyon). The separation of these two components appears insignificant. The suggested peaks in the differential emission measure distribution between 2 and 6 MK are probably not statistically significant: a single, broad feature in the $T\varphi(T)$ distribution would yield a fit to the observed spectrum that is equally acceptable. This double peak may correspond to the 5 MK components seen in the spectra of Capella and σ^2 CrB.

VI. DISCUSSION AND SUMMARY

The analysis of the X-ray spectra of Capella, σ^2 CrB, and Procyon demonstrates that a few, relatively narrow temperature intervals dominate their coronae. In fact, a comparison by eye of a two-temperature fit and of a complete differential emission measure analysis of the observed spectra shows only small differences, although the formal acceptance levels of the multitemperature fits are much higher than those of the two-temperature fits (compare Tables 2 and 3). In Capella and σ^2 CrB the predominant temperatures are 5 MK and $\sim$25 MK, in Procyon 0.6 MK. Note that the predominant temperatures are the same in the dwarf σ^2 CrB as in the giant Capella.

The 5 MK component is seen on all three stars, although Procyon may have a somewhat lower value of 3 MK. We tentatively identify this component with common solar features: Schrijver *et al.* (1984), for example, show that temperatures for loops over solar bipolar regions lie between 2 MK observed for stars could be due entirely to the use of different spectral diagnostics and atomic data.
sation over solar bipolar regions is slightly lower than the 5 MK observed for stars could be due to entirely to the use of different spectral diagnostics and atomic data.

The stellar 25 MK component on stars may not have a quiescent solar counterpart, although Schadee (1983) reports that observations made with the HXIS instrument on *Solar Maximum Mission* show very weak, small, but long-lived features with temperatures in excess of 10 MK. The nature of these hot features is still unclear. With this one exception, temperatures as high as 25 MK are observed on the Sun only in flares. The stellar 25 MK component may be related to stellar flares, in which case the generally featureless X-ray light curves of Capella and σ^2 CrB (Fig. 4) would require a large number of small flares.

The differential emission measure results for Capella and σ^2 CrB agree with the tentative conclusion from Paper II that two temperature components dominate the coronae of cool G- and K-type stars. These two temperatures may be the same in all stars, while different emission measures ratios for the two components result in different characteristic coronal temperatures (as derived from single-temperature fits to *HEAO 2* IPC spectra) in different stars. Paper II suggested that the ratio of emission measures for the two temperature components depends on the stellar level of activity and on the surface gravity of the star, while other parameters may also be involved. Our present results support this conclusion.

The 0.6 MK component of Procyon (F5 IV–V), absent on Capella and σ^2 CrB, also lacks a clear solar counterpart. Such a cool coronal component may be a common phenomenon for

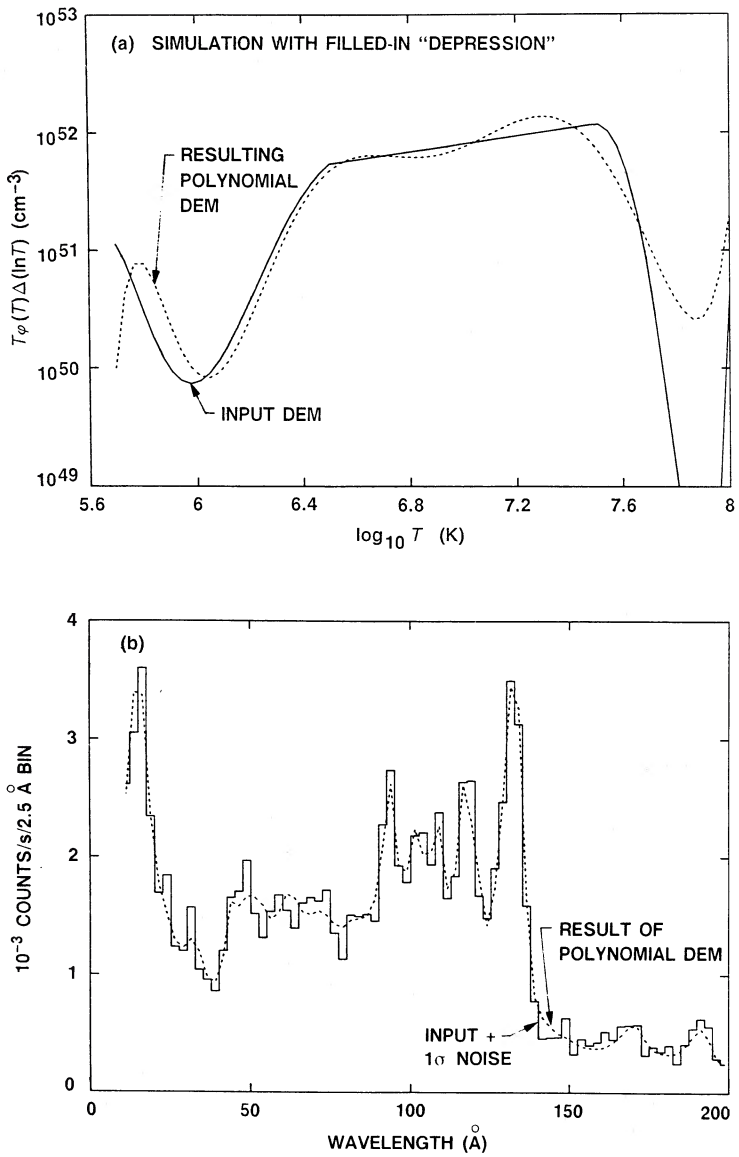

FIG. 8.—Simulations of the Capella spectrum (*a*) with the "depression" in the differential emission measure (*DEM*) distribution around 10 MK filled in [*solid curve*; compare with Fig. 6*a*; again $\Delta \ln(T) = 0.081$]. Panel (*a*) also gives the *DEM* resulting from a spectral analysis (using the "polynomial" [*P*] method) of the spectrum associated with the artificial *DEM*, with 1 σ noise added (*dotted*) to the spectrum. Panel (*b*) compares the spectrum generated using the filled-in *DEM* (*full-drawn*), and spectrum resulting from the "polynomial" *DEM* analysis (*dotted*).

early F-type stars (Walter 1987). Perhaps the properties of the thin F-star convective zone result in a distinct, cool coronal component. Schrijver (1987) suggests that the atmospheric emission of cool stars comprises two components: (i) an emission associated with plasma heated by magnetohydrodynamic effects, and (ii) an emission that is independent of the stellar magnetic activity, the so-called "basal" component. It has been suggested that the basal component is caused by acoustic heating which is strongest in the early F-type stars. One could conjecture that the cool 0.6 MK component is related to the strong basal fluxes in early F-type stars. Schrijver (1987) does not find clear evidence for a basal flux in X-ray observations, but this could be caused by a rapid decrease of the basal X-ray flux with effective stellar temperature, so that a possible basal coronal component in the cooler G- and K-type stars in his sample is masked by brighter emission produced by magnetically heated plasma.

The existence of three dominant temperatures in the coronae of cool stars may reflect different heating mechanisms for the three components, or contain information on the stability of the corresponding loops, or both. It is noteworthy that the three dominant temperatures correspond with temperature intervals in which the coronal radiative loss $\Lambda(T)$ increases with increasing temperature (Fig. 1 in Mewe, Gronenschild, and van den Oord 1985). The gradients in $\Lambda(T)$ are small around the temperatures that dominate the stellar spectra. If radiation is the dominant cooling mechanism, the apex loop temperatures may tend toward values that make the loop relatively insensitive to heat fluctuations. The avoidance of decreasing sections of $\Lambda(T)$ may be more significant: the gra-

dients in $\Lambda(T)$ in these intervals are stronger, so that the coronal plasma is possibly unstable to fluctuations.

The steep increase with temperature of the differential emission measure distributions $T\varphi(T)$ derived for Capella and σ^2 CrB shows that the model for static magnetic loops, as developed by Rosner, Tucker, and Vaiana (1978, RTV), is incompatible with the data (see discussion in Schrijver, Lemen, and Mewe 1988; Paper IV). This steep increase in differential emission measure $T\varphi(T)$ below 3 MK may imply that the geometry of the loop differs distinctly from the constant cross-section loops of the RTV model. For example, if the loops are much wider at the top than at the footpoints, the resulting spectrum will appear to be nearly isothermal. The observed doubly peaked differential emission measure distribution for Capella and σ^2 CrB would then imply a corona consisting of two families of loops with maximum temperatures around 5 MK and 25 MK. In Paper IV we make a detailed two-component analysis of the spectra of Capella and σ^2 CrB, using model coronae comprising two ensembles of loops each characterized by a maximum temperature and a distinct geometry.

Part of the research described in this paper was made possible by the support of the Space Research Organization of the Netherlands (SRON). C. J. Schrijver is supported in part by NASA grant NAG5-82 to the University of Colorado, and acknowledges a visitor grant from the Netherlands Organization for the Advancement of Pure Scientific Research (ZWO). J. R. Lemen acknowledges support received from the U.K. Science and Engineering Research Council, NASA grant NAS5-30431, and the Lockheed Independent Research Program. A. Fludra acknowledges a grant from the British Council. We thank J. M. Braun for assistance in preparing some of the figures.

REFERENCES

Allen, C. W. 1973, in *Astrophysical Quantities* (3d ed.; London: Athlone).
Brinkman, A. C., *et al.* 1980, *Appl. Optics*, **19**, 1601.
Brinkman, A. C., Gronenschild, E. H. B. M., Mewe, R., McHardy, I., and Pye, J. P. 1985, *Adv. Space Res.*, **5**, Nr. 3, 65.
Bruner, M. E., Brown, W. A., Fludra, A., Lemen, J. R., Mason, H. E., and McWhirter, R. W. P. 1989, *Solar Phys.*, in preparation.
Craig, I. J. D., and Brown, J. C. 1976*a*, *Nature*, **264**, 340.
———. 1976*b*, *Astr. Ap.*, **49**, 239.
de Korte, P. A. J., *et al.* 1981, *Space Sci. Rev.*, **30**, 495.
Dupree, A. K. 1981, *Space Sci. Rev.*, **29**, 479.
Fludra, A., and Sylwester, J. 1986, *Solar Phys.*, **105**, 323.
Gorenstein, P., Harnden, F. R., Jr., and Fabricant, D. G. 1981, *IEEE Trans.*, **NS-28**, 869.
Hoffleit, D., and Jaschek, C. 1982, in *Catalogue of Bright Stars* (4th ed.; New Haven: Yale University Observatory).
Jakimiec, J., *et al.* 1984, *Adv. Space Res.*, **4**, No. 7, 203.
Kastner, S. O., Neupert, W. M., and Swartz, M. 1974, *Ap. J.*, **191**, 261.
Levine, R. H., and Pye, J. P. 1980, *Solar Phys.*, **66**, 39.
Majer, P., Schmitt, J. H. M. M., Golub, L., Harnden, F. R., Jr., and Rosner, R. 1986, *Ap. J.*, **300**, 360.
Mason, H. E., Bhatia, A. K., Kastner, S. O., Neupert, W. M., and Swartz, M. 1984, *Solar Phys.*, **92**, 199.
Mewe, R. 1972, *Solar Phys.*, **22**, 459.
———. 1984, in *Proc. 8th Internat. Colloquium on EUV and X-ray Spectroscopy of Astrophysical and Laboratory Plasmas* (*IAU Colloquium* **86**) (Washington, DC: Naval Research Laboratory), p. 59.
Mewe, R., and Gronenschild, E. H. B. M. 1981, *Astr. Ap. Suppl.*, **45**, 11.
Mewe, R., *et al.* 1982, *Ap. J.*, **260**, 233.
Mewe, R., Gronenschild, E. H. B. M., and van den Oord, G. H. J. 1985, *Astr. Ap. Suppl.*, **62**, 197.
Mewe, R., Lemen, J. R., and van den Oord, G. H. J. 1986, *Astr. Ap. Suppl.*, **65**, 511.
Mewe, R., Schrijver, C. J., Lemen, J. R., and Bentley, R. D. 1986, *Adv. Space Res.*, **6**, No. 8, 133.
Paresce, F. 1984, *A.J.*, **89**, 7.
Rosner, R., Tucker, W. M., and Vaiana, G. S. 1978, *Ap. J.*, **220**, 643 (RTV).
Schadee, A. 1983, *Solar Phys.*, **89**, 287.
Schmitt, J. H. M. M., Harnden, F. R., Jr., Peres, G., Rosner, R., and Serio, S. 1985, *Ap. J.*, **288**, 751.
Schrijver, C. J. 1985, *Space Sci. Rev.*, **40**, 3.
———. 1987, *Astr. Ap.*, **172**, 111.
Schrijver, C. J., and Mewe, R. 1986, in *Cool Stars, Stellar Systems, and the Sun*, ed. M. Zeilik and D. M. Gibson (New York: Springer), p. 300.
Schrijver, C. J., Mewe, R., and Walter, F. M. 1984, *Astr. Ap.*, **138**, 258 (Paper II).
Schrijver, C. J., Lemen, J. R., and Mewe, R. 1989, *Ap. J.*, in press (Paper IV).
Schrijver, C. J., Zwaan, C., Maxson, C. W., and Noyes, R. W. 1984, *Astr. Ap.*, **149**, 123.
Sylwester, J., Schrijver, J., and Mewe, R. 1980, *Solar Phys.*, **67**, 285.
Swank, J. H., White, N. E., Holt, S. S., and Becker, R. H. 1981, *Ap. J.*, **246**, 208.
Tarafdar, S. P., and Agrawal, P. C. 1984, *M.N.R.A.S.*, **207**, 809.
Turner, M. J. L., Smith, A., and Zimmermann, H. V. 1981, *Space Sci. Rev.*, **30**, 513.
van den Oord, G. H. J., Mewe, R., and Brinkman, A. C. 1988*a*, *Astr. Ap.*, **205**. 181.
van den Oord, G. H. J., Mewe, R., and Brinkman, A. C. 1988*b*, in *Cool Stars, Stellar Systems, and the Sun*, ed. J. L. Linsky and R. E. Stencel (New York: Springer), p. 494.
Walter, F. M. 1987, private communication.
Withbroe, G. L. 1975, *Solar Phys.*, **45**, 301.

A. FLUDRA: Mullard Space Science Laboratory, Holmbury St. Mary, Dorking, Surrey RH5 6NT, England

J. R. LEMEN: Lockheed Palo Alto Research Laboratory, Dept. 91-30, 3251 Hanover Street, Palo Alto, CA 94304

R. MEWE: Laboratory for Space Research, Beneluxlaan 21, 3527 HS Utrecht, The Netherlands

C. J. SCHRIJVER: Joint Institute for Laboratory Astrophysics, University of Colorado and National Bureau of Standards, Boulder, CO 80309-0440